HHS Public Access

Author manuscript

J Org Chem. Author manuscript; available in PMC 2018 May 18.

Published in final edited form as:

J Org Chem. 2009 February 20; 74(4): 1440–1449. doi:10.1021/jo8023363.

Synthesis and Characterization of Nitroaromatic Peptoids: Fine Tuning Peptoid Secondary Structure Through Monomer Position and Functionality

Sarah A Fowler, **Rinrada Luechapanichkul**, and **Helen E Blackwell***

Department of Chemistry, University of Wisconsin–Madison, 1101 University Avenue, Madison, WI 53706-1322

Abstract

N-substituted glycine oligomers, or peptoids, have emerged as an important class of foldamers for the study of biomolecular interactions and for potential use as therapeutic agents. However, the design of peptoids with well-defined conformations *a priori* remains a formidable challenge. New approaches are required to address this problem, and the systematic study of the role of individual monomer units in the global peptoid folding process represents one strategy. Here, we report our efforts toward this approach through the design, synthesis, and characterization of peptoids containing nitroaromatic monomer units. This work required the synthesis of a new chiral amine building block, (*S*)-1-(2-nitrophenyl)ethanamine (s2ne), which could be readily installed into peptoids using standard solid-phase peptoid synthesis techniques. We designed a series of peptoid nonamers that allowed us to probe the effects of this relatively electron-deficient and sterically encumbered α-chiral side chain on peptoid structure, namely, the peptoid threaded loop and helix. Circular dichroism (CD) spectroscopy of the peptoids revealed that the nitroaromatic monomer has a significant effect on peptoid secondary structure. Specifically, the threaded loop structure was disrupted in a nonamer containing alternating *N*-(*S*)-1-phenylethylglycine (*N*spe) and *N*s2ne monomers, and the major conformation was helical instead. Indeed, placement of a single *N*s2ne at the *N*-terminal position of $(N\text{spe})_9$ resulted in a destabilized form of the threaded loop structure relative to the homononamer $(N\text{spe})_9$. Conversely, we observed that incorporation of *N*-(*S*)-1-(4-nitrophenyl)ethylglycine (*N*snp, a *para*-nitro monomer) at the *N*-terminal position *stabilized* the threaded loop structure relative to $(N\text{spe})_9$. Additional experiments revealed that nitroaromatic side chains can influence peptoid nonamer folding by modulating the strength of key intramolecular hydrogen bonds in the peptoid threaded loop structure. Steric interactions were also implicated for the *N*s2ne monomer. Overall, this study provides further evidence that aromatic side chain structure, even if perturbed in a single monomer unit, can strongly influence local peptoid backbone conformation.

Abstract

*To whom correspondence should be addressed.

Supporting Information Available

General experimental information, crystallographic information file for acetamide **6**, full X-ray data for **6**, HPLC data for peptoids **2** and **8**–**10**, and NMR data for amine **5b** and peptoids **2**, **7**, and **9**. This material is available free of charge via the Internet at http://pubs.acs.org.

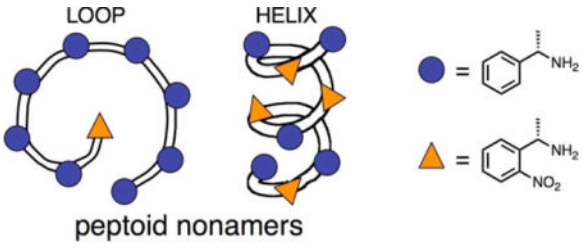

Introduction

Oligomers of *N*-substituted glycine, or peptoids, represent a versatile class of peptidomimetics for the study of biomolecular phenomena.[1] Peptoids are attractive for at least three reasons, including (1) their ease of synthesis, (2) their proteolytic stability, and (3) the wide variety of non-native functionality that can be incorporated into their amide side chains. These features have prompted the development of peptoids as tools to probe a diverse range of biological processes and as therapeutic agents. Recent examples include peptoid-derived transcription factor mimics,[2] protein-protein interaction inhibitors,[3] antimicrobial agents,[4] and lung surfactant mimics.[5] An underlying theme in the majority of these studies has been the connection between peptoid function and peptoid structure.[6] For certain applications, well-folded peptoids are essential for activity, while unstructured peptoids appear to suffice, or even are superior, for other applications.[3,4] These structure-function connections are largely made after the design, synthesis, and characterization process. The future development of peptoids as chemical tools will require an ability to determine the applications for which structured peptoids are or are not required, and simultaneously, the development of straightforward *de novo* design strategies to generate structured peptoids. Conformational heterogeneity arising from backbone amide isomerism, however, has significantly complicated the design of well-folded peptoid structural motifs, and the current understanding of the peptoid folding process remains at a formative stage.

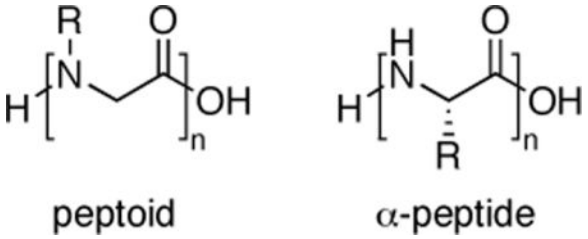

In contrast to the α-peptide backbone, peptoid backbones lack both chiral centers and hydrogen bond donors, and this, coupled with facile tertiary amide isomerism, reduces the conformational rigidity of peptoids. One strategy to enforce more predictable peptoid folding is the “reinstallation” of chiral centers or hydrogen bond donors into peptoid side chains, and the former approach has been particularly fruitful for the construction of peptoid helices.[7] Namely, the inclusion of α-chiral aromatic or α-chiral aliphatic amide side chains in peptoids enforces a helical conformation reminiscent of a polyproline type-I helix, with all *cis*-amide bonds and three residues per turn (Figure 1A). The peptoid helix was first reported by Barron, Kirshenbaum, Dill, Zuckermann, and co-workers, and has been

characterized by computational techniques, circular dichroism (CD) spectroscopy, X-ray crystallography, and 2D NMR.[7,8] Most peptoid helices are composed primarily of (*S*)-*N*-(1-phenylethyl)glycine units (*N*spe, Figure 1), and are commonly identified by a diagnostic CD signature with minima at 192, 202, and 218 nm. Through the analysis of *N*spe-type oligomers of various lengths and compositons,[7b,9] Barron and co-workers developed a set of predictive rules for peptoid helix formation. In brief, oligomers containing 50% α-chiral side chains or an "aromatic face" running down the longitudinal face of the helix (*i.e.*, aromatic side chains in a three-fold periodic pattern) are predicted to form the most stable helices, and these helices are further stabilized when the *C*-terminal residue is α-chiral and at oligomer lengths beyond 12 residues. These rules have proven valuable in the recent design of peptoid mimics of various naturally occurring α-peptide helices.[4,5]

Through careful study of the peptoid helix, Barron and co-workers uncovered a new peptoid structure in 2006, the threaded loop (shown in Figure 1B).[10] This discovery was significant, as up until this point, the peptoid helix was the only known, defined secondary structure for peptoids. A peptoid nonamer of α-chiral aromatic side chains, (*N*spe)$_9$ (**2**, evaluated as the trifluoroacetic acid salt), was found to display a unique CD signature in acetonitrile, with a single broad peak of significant intensity at 203 nm.[7b] Further analysis of **2** by 2D NMR techniques in acetonitrile-d_3 revealed that it adopted a well-defined loop-like structure. The loop was stabilized by three intramolecular hydrogen bonds from backbone carbonyls (residues 5, 7, and 9) to the *N*-terminal secondary ammonium and one intramolecular hydrogen bond from a backbone carbonyl (residue 2) to the *C*-terminal primary amide (Figure 1B).[10] In contrast to the peptoid helix (Figure 1A), the threaded loop structure has four *cis* and four *trans* amide bonds. As only the *N*spe nonamer **2** and nonamers with closely related α-chiral residues are able to form the threaded loop, this oligomer length appears poised to compact itself and form the four intramolecular hydrogen bonds. Indeed, *N*spe pentamers to octamers and decamers to longer oligomers all show a heightened propensity for helix formation over threaded loop formation,[7b] indicating that the molecular contacts necessary for threaded loop formation are unique to nine residue long peptoids. Notably, the threaded loop in **2** can be converted back to a helix by addition of a solvent capable of disrupting the intramolecular hydrogen bonds (*e.g.*, methanol), suggesting that the loop and helix are endpoints on a conformational continuum for this nonamer class.[10]

Beyond the threaded loop and helix, turn motifs have been recently reported in peptoids, achieved either by macrocyclization[12] or by incorporation of a turn-inducing triazole unit.[13] These motifs certainly expand the repertoire of known peptoid structures, and their applications in peptoid research are now being delineated. Additional research is necessary, however, to expand our understanding of the molecular level interactions that are necessary for peptoid folding into helices, loops, turns, and beyond. These structures are currently reserved to a relatively small set of peptoid primary sequence space. A major goal of our research is to develop new and robust approaches to construct discretely folded peptoids through the strategic installation of functionality capable of non-covalent interactions,[14] starting at the most basic monomer level[15] and building to more complex, oligomeric structures.[16,17] We report herein our recent efforts toward this goal through a systematic study of peptoids containing α-chiral nitroaromatic monomers.

In 2005, we reported the design and synthesis of a peptoid nonamer of alternating α-chiral aromatic (*N*spe) and achiral nitroaromatic (*N*-1-(2-nitrophenylethyl)glycine, *N*2nb) monomer units.[14] The CD signature of this alternating heterononamer indicated that it adopted a helical structure in acetonitrile, with intensities analogous to that of helical *N*spe octamer and decamer peptoids (evaluated as the mirror image *N*rpe systems).[7b] Again, the *N*spe *homononamer* **2** adopts a threaded loop as opposed to a helix. We initially postulated that the pattern of more electron-rich (*N*spe) and more electron-poor aromatic side chains (*N*2nb) along each of the heterononamer helix faces could stabilize a helical conformation relative to the threaded loop due to potential intramolecular quadrupolar interactions between side chains on each face of the helix. Later studies, however, indicated that such quadrupolar interactions are most likely not a major contributor to helix stabilization,[16] and we sought to further investigate the origin of helix stabilization in this peptoid system. We reasoned that a more direct comparison could be made between this nitroaromatic heterononamer and $(N\text{spe})_9$ **2** if the *N*2nb side chains were also α-chiral. Therefore, to perform this experiment, we required (*S*)-1-(2-nitrophenyl)ethanamine (s2ne) as a new chiral amine building block for peptoid synthesis.

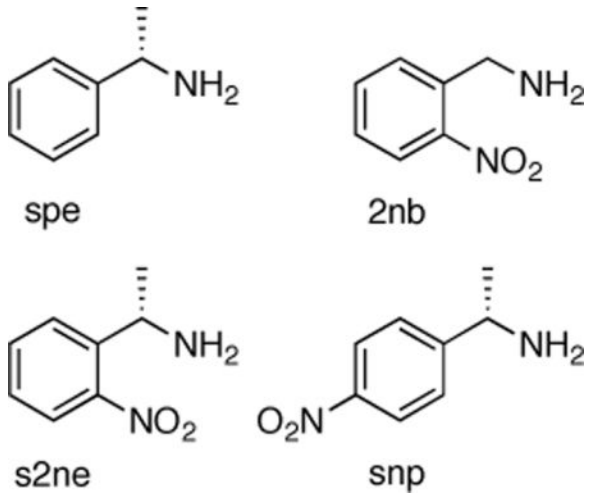

Simultaneous to our analysis of nitroaromatic peptoids, our lab also has been studying the effects of single amide side chain mutations on peptoid helix and threaded loop structure in *N*spe-type systems. We recently reported the incorporation of (*S*)-*N*-(1-pentafluorophenylethyl)glycine (*N*sfe) at specific positions in α-chiral peptoid nonamers,[16] and observed that either helical or threaded loop structure could be promoted depending on the position at which the substituted side chain was incorporated. This outcome was attributed to the electron-withdrawing effect of the pentafluoroaromatic side chain on adjacent backbone amide carbonyls and the ammonium terminus, and thus the ability to weaken or strengthen hydrogen bonds in the threaded loop structure (at positions 3, 6, and 8 or 1, respectively; Figure 1B). In addition, other sites were found to be perturbed by pentafluoroaromatic substitution (positions 2 and 5), suggesting that additional amide carbonyls also may participate in hydrogen bonding in the threaded loop. We desired to examine the generality of this “mutational” approach, and within the context of the current study, sought to incorporate electron-withdrawing nitroaromatic side chains at key positions

to further probe the stability of the hydrogen bonds in the threaded loop structure. Specifically, we were interested in enhancing the hydrogen bonding capacity of the ammonium terminus (position 1) in peptoid nonamers, as this was shown to significantly *stabilize* the threaded loop structure.[16]

Herein, we report the synthesis of (*S*)-1-(2-nitrophenyl)ethanamine (s2ne, **5b**), the design and construction of peptoid nonamers containing this chiral amine, and the structural characterization of the nonamer products by CD and NMR spectroscopy. First, we synthesized a heteropeptoid of alternating *N*spe and *N*s2ne units to compare to our previous work. Characterization of this nonamer by CD spectroscopy revealed that a helical conformation induced by nitroaromatic side chains is further stabilized when all side chains are α-chiral. This result provides further support for the set of rules for helix stabilization developed by Barron and co-workers,[9] and extends it to a nitro-functionalized aromatic side chain. Second, we synthesized and studied *N*spe heterononamers with *N*s2ne and the 4-substituted analog, (*S*)-1-(4-nitrophenyl)ethylglycine (*N*snp),[18] at the *N*-termini. These single monomer mutations allowed us to probe the effects of a nitroaromatic side chain on the hydrogen bond from the *N*-terminal ammonium to residues 5, 7, and 9 in the threaded loop structure. Both of these nonamers were observed to adopt a threaded loop conformation in acetonitrile. However, the inclusion of *N*s2ne caused the nonamer structure to be significantly destabilized relative to the canonical threaded loop for $(N\text{spe})_9$ (**2**), while the *N*snp-containing nonamer was stabilized. Overall, our findings suggest that peptoid folding can be controlled by subtle structural alterations to individual monomer units, some as simple as the position of a functional group on one aromatic ring (*ortho* v. *para)*. These results suggest a pathway not only for the stabilization of known peptoid structures, but also for the future design of new structural motifs.

Results and Discussion

Synthesis of (*S*)-1-(2-nitrophenyl)ethanamine (s2ne)

Nitrophenylethylamines have been used for the chiral resolution of organic compounds for over 30 years,[19] and several synthetic routes have been pursued for their preparation. Syntheses of racemic 1-(2-nitrophenyl)ethanamine, either *via* reductive amination of a ketone[20] or borane reduction of an oxime,[21] have been reported previously. A route to enantiopure s2ne or r2ne, to our knowledge, is yet to be reported. Perry *et al.*[19a] reported a straightforward synthetic route to the *para*-nitro analog, (*S)*-1-(4-nitrophenyl)ethylamine, and this amine (snp) is now commercially available. This method involved the nitration of spe with HNO_3, and only the *para*-nitration product was isolated. We sought to modify this nitration method to yield appreciable quantities of the *ortho*-nitration product, s2ne (**5b**), from spe. Our optimized route is shown in Scheme 1.

Similar to Perry *et al.*,[19a] our initial route to **5b** involved protecting spe as the acetamide, and then subsequent nitration with either HNO_3 or HNO_3/H_2SO_4. This procedure only returned starting material acetamide, however.[22] We therefore sought a more reactive nitrating reagent, and in turn, an alternate protecting group for spe. Our final route proceeded as follows. First, spe was protected as the more acid-stable trifluoroacetamide (**3**) under standard conditions (Scheme 1).[23] Thereafter, phenyl nitration was performed by treatment

of **3** with the highly reactive electrophile $CF_3SO_2^-NO_2$ generated from nitric and triflic acid. The nitration product was obtained in 92% yield as a 3:2 ratio of *para* and *ortho* isomers (**4a** and **4b**). (We note that nitro compounds **4**–**6** are susceptible to degradation by light and were handled and stored in the dark throughout this study.) The separation of regioisomers **4a** and **4b** by column chromatography proved difficult, and we therefore examined replacing the trifluoroacetyl[24] with other amine protecting groups to aid separation (*e.g.*, Boc, Fmoc, and acetyl). We found that the acetylated mixture of **5a** and **5b** could be easily separated by recrystallization from ethyl acetate, allowing for the isolation of the *ortho*-NO_2 acetamide (**6**) in nearly quantitative yield and >95% purity.[25] To complete the synthesis of s2ne, acetamide **6** was deprotected to yield the amine hydrochloride salt **5b** in 35% overall yield from spe. We found this synthetic route to be highly robust, and we isolated **5b** routinely on a 200 mg scale. Notably, nitroaromatic amine **5b** should prove useful not only for peptoid synthesis, but also as new chiral building block for other synthetic applications.

During the course of our synthetic work, we obtained an X-ray crystal structure of *ortho*-nitro acetamide **6** (shown in Figure 2). The molecules were arranged in the $P4_3$ space group, a tetrad repeat in which each molecule is rotated 90° relative to the neighboring molecule. Intermolecular hydrogen bonds were present between adjacent amide protons and amide oxygens. The crystal structure not only confirmed the identity of acetamide **6**, but also highlighted the hydrogen-bonding capability of this class of nitro aromatic compound. We reasoned this property could influence the folding of peptoid oligomers containing s2ne (**5b**), most notably those with a propensity to adopt a threaded loop.

Peptoid Design

We previously reported that an alternating heterononamer of *N*spe and *N*2nb (**7**) exhibited a helical CD signature in acetonitrile (see above).[14] However, the comparison of heterononamer **7** to $(N\text{spe})_9$ (**2**) was not ideal, as **7** contains only five α-chiral side chains as opposed to the nine in **2**. The number of chiral centers in a molecule will influence the intensity of its CD spectrum, and the inclusion of α-chiral side chains in peptoids is well documented to rigidify their structures, whether helical or threaded loop (see above). Therefore, our first design goal was to generate an alternating heterononamer of *N*spe and *N*s2ne units, *i.e.*, $N\text{spe}(N\text{s2ne}N\text{spe})_4$ (**8**), to compare to homononamer **2** and heterononamer **7** by CD spectroscopy.

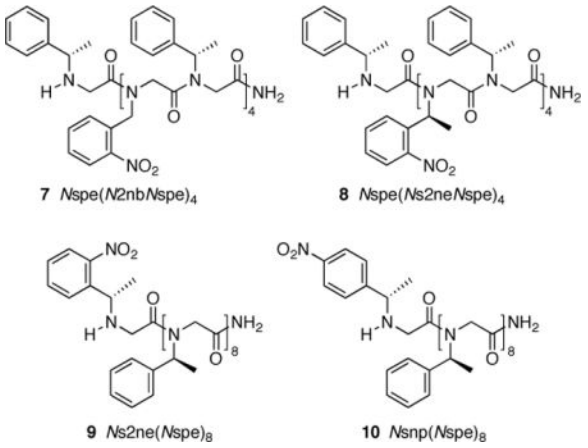

The second goal of our peptoid design was to further probe the effects of tuning the hydrogen bonding capability of the *N*-terminal ammonium in the peptoid threaded loop. We reasoned that inductive withdrawal of electron density at this terminus by a pendant nitroaromatic group could likely increase the acidity of the ammonium group, and thus increase its hydrogen bonding potential. We consequently designed *N*spe nonamers with single *ortho*-nitro monomer *N*s2ne or *para*-nitro monomer *N*snp replacements at the *N*-termini (*N*s2ne(*N*spe)$_8$ **9** and *N*snp(*N*spe)$_8$ **10**, respectively). Electron density would be removed from the *N*-terminal ammonium in both nonamers. However, the *ortho*-nitroaromatic group should engender stronger inductive effects in peptoid **9** relative to those in *para*-nitroaromatic peptoid **10**. We reasoned that the *ortho*-nitro group in peptoid **9** could also have altered steric contacts in the threaded loop structure relative to peptoid **10** and the homononamer **2**, and this could play an additional role in the conformation adopted by peptoid **9**.[26]

Peptoid Synthesis

We synthesized (*N*spe)$_9$ **2** (for use as a control) and peptoid nonamers **8**–**10** on Rink-amide linker derivatized polystyrene resin using a modified version of our previously reported, microwave (μW)-assisted peptoid synthesis method (shown in Scheme 2).[14] Heterononamer **7** was synthesized using a similar sub-monomer synthesis method; we utilized a sample of **7** from our earlier work as a control for this study.[14]

To build each peptoid monomer unit, bromoacetic acid was coupled to the resin-supported amine (μW 30 sec, 35 °C), followed by displacement of the bromide with a primary amine (spe, s2ne (**5b**), or snp; μW 90 sec, 95 °C; Scheme 2). Notably, we observed decreased yields and crude purities for the peptoids constructed from α-chiral nitroaromatic amines (s2ne (**5b**) and snp), most probably due to the decreased nucleophilicities of these amines.[14] Careful reaction optimization revealed that μW heating for 1 h at a reduced temperature (60 °C) was beneficial for incorporation of these amines; for example, the crude purity of nonamer **9** was 13% using standard μW conditions, and increased to 20% with a longer heating time. This modified amination method was therefore used to incorporate the nitroaromatic amines into peptoids **8**–**10**. After acid-mediated resin cleavage, peptoids **2** and **8**–**10** were purified to homogeneity (>95%) by preparative RP-HPLC to yield ~2–5 mg of

each peptoid. The purities and identities of the purified peptoids were confirmed by analytical RP-HPLC (see Supporting Information) and mass spectrometry (Table 1). Peptoids containing nitroaromatic side chains were manipulated and stored in the dark throughout this study to minimize the chance of photodecomposition.

CD Characterization of Peptoids 7 and 8

The secondary structures of the alternating nonamer peptoids **7** and **8** were evaluated by CD spectroscopy in the first phase of this study (Figure 3). We observed that peptoid **8** containing all α-chiral residues (*N*spe and *N*s2ne) displayed a CD signature indicative of helicity in acetonitrile, and this signature was qualitatively similar in shape and intensity to that for peptoid **7** containing only ~50% α-chiral residues (*i.e.*, five *N*spe and four *N*2nb). We note that both peptoids **7** and **8** have *ortho*-nitroaromatic amide side chains at positions 2, 6, and 8, and that the adjacent amide carbonyls (at positions 1, 5, and 7) act as hydrogen bond acceptors in the canonical threaded loop structure (see Figure 1B). The electron-withdrawing nitroaromatic groups could be weakening these adjacent hydrogen bonds, and thus destabilizing threaded loop structure and, in turn, enforcing helical structure in peptoids **7** and **8**. The spectrum of nonamer **8** more closely resembled the spectrum of a peptoid helix than that of a loop, with a minimum at 218 nm of slightly greater intensity than the minimum at 202 nm. In fact, the shape and intensity of the spectrum of nonamer **8** was very similar to the previously reported spectrum of the *N*rpe heptamer, which was interpreted as a representation of multiple conformations, of which the major conformer was the peptoid helix.[7b]

The CD spectrum for peptoid **7**, in contrast to that for **8**, had a minimum at 218 nm that was moderately *lower* in intensity relative to the minimum at ~202 nm (Figure 3). This pattern of intensities is not a common observation for peptoid helices. Indeed, a single broad peak of significant intensity at 203 nm is actually indicative of the threaded loop (see above),[7b] suggesting that peptoid **7** could also sample this conformation in acetonitrile. To gain further insight into the structure of peptoid **7**, we evaluated this nonamer by NMR spectroscopic techniques in acetonitrile-d_3 at 24 °C (see Supporting Information). We observed many overlapping resonances that were poorly resolved in the 1D ^{1}H NMR spectrum of **7**, suggesting multiple conformations were present in solution. We next sought to evaluate the ratio of *cis* and *trans* amide bonds in **7** using heteronuclear single quantum coherence (HSQC) NMR; unfortunately, the low solubility of **7** in acetonitrile-d_3 precluded us from obtaining an acceptable HSQC spectrum due to low signal strength. Instead, we chose to evaluate **7** in DMSO-d_6, which allowed us to prepare a more concentrated sample.[27] The 1D ^{1}H NMR spectrum of **7** in DMSO-d_6 displayed more overlapping resonances than the spectrum in acetonitrile-d_3, with approximately the same level of resolution. The HSQC spectrum of peptoid **7** in DMSO-d_6 contained multiple resonances for the benzylic protons, and we observed an approximately 5:1 *cis*:*trans* ratio of amide rotamers (by integration of benzylic protons; see Experimental Section for details of NMR experiment). These data suggested that more than one conformer of **7** was present in both acetonitrile and DMSO solutions. Based on these CD and NMR results, we deduce that peptoid **7** has a moderately lower propensity for a helical conformation relative to peptoid **8**. This result is in accord with the helix stabilization rules outlined by Barron and coworkers: that is, the higher the

percentage of α-chiral residues in a peptoid helix, the more stable the helical structure.[7b,9] Another important outcome from this study is our demonstration that the inclusion of multiple *ortho*-nitroaromatic amide side chains, whether α-chiral or not, can stabilize helical structure relative to loop structure in peptoid nonamers.

CD Characterization of Peptoids 9 and 10

We initiated the second phase of this study by characterizing peptoid heterononamers **9** and **10** by CD spectroscopy. We expected to see a strengthening of the threaded loop structure in peptoids **9** and **10**, each with an α-chiral nitroaromatic amide side chain at position 1, due to strengthening of hydrogen bonds to the presumably more acidic *N*-terminal ammoniums in these peptoids. In accord with previous interpretations of CD spectra in the peptoid field, we looked for an increase in CD peak intensity as an indication of increased structural stability.[7,9] We compared the CD spectra of peptoids **9** and **10** to the CD spectrum of the canonical threaded loop, (*N*spe)$_9$ (**2**), in acetonitrile (Figure 4). Indeed, the spectrum of nonamer **10**, containing *N*snp at position 1, showed a 30% increase in intensity at 203 nm relative to the spectrum of **2** (albeit slightly shifted to lower wavelength (~201 nm)),[28] suggesting that the threaded loop structure was stabilized in this peptoid relative to **2**. We attributed this increase in loop stability in **10** to strengthened hydrogen bonding to the *N*-terminal ammonium, as a result of the electron-withdrawing *para*-nitroaromatic side chain at position 1. Such a stabilization effect is congruent with our previous results for the incorporation of a pentafluoroaromatic amide side chain (*N*sfe) at position 1 in an *N*spe nonamer (see above).[16]

In contrast to peptoid **10**, we observed a weakening of the CD signature for nonamer **9** containing the *ortho*-nitroaromatic monomer (*N*s2ne) at position 1 relative to nonamer **2** (Figure 4). The minimum was shifted to 208 nm and was ~4-fold less intense than **10**, and the overall signature was significantly broader than that for either **10** or **2**. A rationale for loop *destabilization* in peptoid **9** due to an inductive effect was not immediately apparent. Careful examination of the reported 3D structure of the threaded loop for **2** (see Figure 1B) revealed that an *ortho*-substituent in the position 1 amide side chain may have unfavorable steric interactions with both the backbone and side chains in the loop (*e.g.*, the amide carbonyls at residues 5 and 7 and α-methyl at residue 9).[29] Unfavorable steric interactions between the *ortho*-nitro group and the α-methyl group within the *N*s2ne monomer should also be considered. The side chain could adopt a dihedral angle that avoids this interaction, which could potentially torque the ammonium hydrogens away from the backbone acceptor carbonyls and thereby weaken threaded loop structure in **9**. In addition to these potential interactions, we cannot discount the potential for the formation of a H-bond between the *ortho*-nitro and the *N*-terminal ammonium, which would again limit the ammonium's ability to stabilize the threaded loop. But, interestingly, we did not observe a CD spectrum for **9** indicating helical structure in acetonitrile. If the *ortho*-nitro group was preventing peptoid **9** from folding into a threaded loop, it was not reverting to a helical conformation. Rather, the overall shape of the CD spectrum for **9** suggested a threaded loop, though the lowered intensity led us to postulate that the structure was not highly stable.

To obtain more insight into the structure of *N*s2ne(*N*spe)$_8$ **(9)**, we acquired CD spectra of **9** in solutions of varying compositions of methanol/acetonitrile (Figure 5). Such solvent titration experiments have been performed previously on nonamer peptoids that adopt the threaded loop structure to probe the relative strength of the intramolecular hydrogen bonds.[10,16] Methanol competes for the intramolecular hydrogen bonds that exist in acetonitrile, and addition of a sufficient quantity of methanol results in conversion of the threaded loop to a helical structure (see above). Our titration study of peptoid **9** revealed a helical CD signature in solutions of ≥10% methanol/acetonitrile. For comparison, a 50% methanol/acetonitrile solution is required to fully disrupt the hydrogen bonds in **2** and observe a helical CD signature.[10,16] Addition of just 10% methanol, however, was sufficient to disrupt the structure of **9** in acetonitrile. Observing this solvent-induced transition, we contend that the structure of peptoid **9** in acetonitrile is similar to the threaded loop, and that it contains intramolecular hydrogen bonds. However, because only a small percentage of methanol was required to disrupt these hydrogen bonds, we infer that they are substantially weakened in peptoid **9** relative to **2**, potentially due to lengthened bonds and/or contorted bond angles.

We performed NMR experiments on nonamer **9** in acetonitrile-d_3 to further examine its structure. The 1D ^{1}H NMR spectrum of **9** was highly similar to the ^{1}H NMR spectrum of (*N*spe)$_9$ (**2**) in acetonitrile-d_3; the dispersion of resonances suggested unique chemical environments for each amide side chain and that **9** adopts one major conformation (see Supporting Information). Integration of the benzylic resonances indicated that there were an approximately equal number of *cis* and *trans* amide bonds in peptoid **9**.[30] The 2D NOESY spectrum for **9** likewise showed resonances for one major conformer (a portion of the spectrum is shown in Figure 6). Integration of the benzylic resonances in the NOESY spectrum indicated a 1.2:1 *trans:cis* amide ratio, or 4.4 *trans*-amides and 3.6 *cis*-amides on average, for peptoid **9** in acetonitrile. This ratio is comparable to that of the canonical threaded loop, **2**, which has approximately four *cis* and four *trans* amides.[10] Based on these NMR and CD experiments, we believe heterononamer **9** adopts a destabilized threaded loop structure in acetonitrile, in which the oligomer is perhaps not as tightly coiled as **2** due to the presence of the *ortho*-nitroaromatic substituent at the *N*-terminus. This “unwinding” of the threaded loop is congruent with our CD solvent titration data for peptoid **9**, indicating significantly weakened intramolecular hydrogen bonding in the nonamer relative to **2**. Such destabilized threaded loop conformations have been proposed previously for homononamers of α-chiral aliphatic side chains.[10]

Together, the results of the second phase of this study indicated that both the structure and position of a substituent on the *N*-terminal aromatic side chain can either dramatically destabilize (*ortho*-nitro) or stabilize (*para*-nitro) the threaded loop. While inductive effects can explain the stabilizing effect of the *para*-nitroaromatic side chain in peptoid **10**, the reasons behind the destabilization of loop structure in the *ortho*-nitroaromatic analog (**9**) are less clear. Our current hypothesis is that this is largely due to a steric effect and/or formation of an H-bond between the nitro group and the *N*-terminus, but we cannot discount other possible inductive effects or electrostatic interactions also. Overall, these results further underscore the dynamic nature of the threaded loop structure, and again, the ability to alter

peptoid secondary structure through seemingly minor structural perturbations to their primary sequence.

Conclusions

We have discovered two new design principles for peptoid folding based on the incorporation of nitroaromatic amide side chains into peptoids. This work was facilitated by the development of a new synthetic route to (*S*)-1-(2-nitrophenyl)ethanamine (s2ne, **5b**), which could be readily incorporated into peptoids using solid-phase methods. First, we showed that the presence of *N*s2ne, or its achiral variant *N*2nb, can destabilize the peptoid threaded loop secondary structure in alternating *N*spe heterononamers (**7** and **8**). CD and NMR experiments revealed that the major conformations of these peptoids were helical, and we postulate that the origin of this effect is destabilization of key hydrogen bonds in the threaded loop structure due to the electron-withdrawing capabilities of the nitroaromatic groups. Second, we demonstrated that the incorporation of a single *N*s2ne at the *N*-terminus of an *N*spe nonamer (**9**) also could destabilize threaded loop structure. Peptoid **9** exhibited a unique CD spectrum in acetonitrile, which further CD and NMR studies indicated to be that of a loosely coiled, threaded loop. In contrast, the *para*-nitro substituted analog of **9** (nonamer **10**) exhibited a significantly *stabilized* threaded loop structure relative to **9** and the canonical threaded loop (**2**), as determined by CD analysis. This latter result is in accord with the strengthened hydrogen bonding capability of the *N*-terminal ammonium in peptoid **10**, and this outcome was also originally anticipated for peptoid **9**. The reasons behind this dramatic shift in loop stability for isomeric peptoids **9** and **10** remain unclear, although we believe that the differing steric effects of *ortho*-nitro versus *para*-nitro groups may play a major role.

To close, this study provides further evidence that peptoid side chain structure, even if perturbed in a single monomer unit, can strongly influence local peptoid backbone conformation. Our results serve to further delineate the direct connections between primary sequence and structure in α-chiral peptoids. Moreover, we demonstrate, to our knowledge, the most exquisite control of peptoid secondary structure reported to date, achievable through highly subtle alterations of amide side chain structure (*i.e.*, the placement of a single functional group on one amide side chain). These results have important implications for the design of new peptoid structures, and for the analysis of previously reported α-chiral peptoids with different substitution patterns and functionality on their aromatic rings. Strategies to stabilize peptoid architectures through minimal side chain perturbations could also prove valuable for the development of functional peptoids. This could permit the installation of a higher percentage of side chains that endow the peptoid with desirable properties (*e.g.*, solubility, cell permeability, or biological activity), as opposed to being restricted largely to those that only enforce structure. Ongoing work in our laboratory is directed toward applying these design strategies to further refine and expand the existing repertoire of peptoid secondary structures, and will be reported in due course.

Experimental Section

2,2,2-trifluoro-*N*-((*S*)-1-phenylethyl)acetamide (3)

(*S*)-(–)-α-methylbenzylamine (spe, 2.130 mL, 16.50 mmol) was dissolved in CH_2Cl_2 (30 mL) and cooled to 0 °C. Pyridine (3.325 mL, 41.26 mmol, 2.5 equiv) was added to the stirring solution of amine, followed by dropwise addition of trifluoroacetic anhydride (2.910 mL, 20.64 mmol, 1.25 equiv) over 30 min.[23] The reaction was allowed to warm to room temperature (rt) and stirred for 3 h. The reaction mixture was poured into 0.5 N HCl (30 mL) and vigorously stirred for 5 min. The layers were separated, and the aqueous layer was extracted with CH_2Cl_2 (3 × 10 mL). The combined organic layers were washed with 0.5 N HCl (20 mL), H_2O (2 × 20 mL), and saturated $NaHCO_3$ (20 mL), and dried through a cotton plug. The organic phase was concentrated and dried *in vacuo* to give trifluoroacetamide **3** as a white powdery solid (3.556 g, 16.37 mmol, 99% yield). TLC in CH_2Cl_2: R_f = 0.66; ^{1}H NMR (300 MHz, $CDCl_3$) δ 7.33 (m, 5H), 6.39 (bs, 1H), 5.15 (p, J = 7.2 Hz, 1H), 1.59 (d, J = 6.9 Hz, 3H); ^{13}C NMR (75 MHz, $CDCl_3$) δ 156.6 (q, J_{CF} = 36.8 Hz), 141.0, 129.2, 128.4, 126.4, 116.1 (q, J_{CF} = 286.7 Hz), 50.0, 21.1; EI MS calc. 217.0, obs. [M^+] 217.1.

2,2,2-trifluoro-*N*-((*S*)-1-(4-nitrophenyl)ethyl)acetamide (4a) and 2,2,2-trifluoro-*N*-((*S*)-1-(2-nitrophenyl)ethyl)acetamide (4b)

Trifluoromethanesulfonic acid (CF_3SO_3H; 2.9 mL, 32.69 mmol, 2 equiv) was dissolved in CH_2Cl_2 (110 mL) and cooled to 0 °C under N_2. HNO_3 (0.74 mL, 16.34 mmol, 1 equiv) was added, and the reaction mixture was stirred for 15 min at 0 °C, after which it was cooled to –78 °C.[23] Trifluoroacetamide **3** (3.55 g, 16.34 mmol) was dissolved in CH_2Cl_2 (30 mL) and slowly added to the cooled reaction mixture over 1 h, followed by a CH_2Cl_2 rinse (10 mL) of the addition funnel. The reaction mixture was stirred at –78 °C for an additional 30 min, and then at –40 °C for 16 h. The yellow-orange reaction mixture was poured into ice (100 g) and stirred vigorously for 5 min. The layers were separated, and the aqueous layer was extracted with CH_2Cl_2 (3 × 25 mL). The organic layers were combined and washed with H_2O (3 × 100 mL), saturated $NaHCO_3$ (100 mL) and H_2O (100 mL), and dried through a cotton plug. The organic phase was concentrated and dried *in vacuo* to give a ~3:2 mixture of **4a** and **4b** as a pale orange solid (4.026 g, 15.35 mmol, 94% combined yield; 57% **4a** and 43% **4b** as determined by ^{1}H NMR integration.). TLC in 20% diethyl ether/toluene: **4a**: R_f = 0.44; **4b**: R_f = 0.50; ^{1}H NMR (300 MHz, $CDCl_3$) **4a**: δ 8.24 (d, J = 8.9 Hz, 2H), 7.50 (d, J = 8.9 Hz, 2H), 6.65 (bs, 1H), 5.22 (p, J = 7.2 Hz, 1H), 1.63 (d, J = 7.2 Hz, 3H); **4b**: δ 7.97 (dd, J = 7.8, 1.2 Hz, 1H), 7.65 (m, 1H), 7.49 (m, 1H), 7.32 (m, 1H), 7.12 (bs, 1H) 5.54 (p, J = 7.2 Hz, 1H), 1.65 (d, J = 7.2 Hz, 3H); ^{13}C NMR (75 MHz, $CDCl_3$) **4a**: δ 156.9 (q, J_{CF} = 37.5 Hz), 148.6, 136.5, 127.2, 124.4, 115.8 (q, J_{CF} = 286.7 Hz), 49.3, 21.5; **4b**: δ 156.7 (q, J_{CF} = 37.0 Hz), 147.7, 134.2, 132.8, 129.2, 128.7, 125.5, 47.6, 20.8; ESI MS calc. 262.0, obs. [M +Na]$^+$ 285.3.

(*S*)-1-(4-nitrophenyl)ethanamine (5a) and (*S*)-1-(2-nitrophenyl)ethanamine (5b)

The mixture of trifluoroacetamides **4a** and **4b** (0.215 g, 0.82 mmol) was dissolved in a 16:1 MeOH:H_2O solution (33 mL). K_2CO_3 (0.572 g, 4.10 mmol, 5 equiv) was added, and the reaction mixture was refluxed with stirring for 16 h.[24] The orange reaction mixture was concentrated *in vacuo* to yield an orange solid, which was dissolved in H_2O (30 mL) and

extracted with $CHCl_3$ (3 × 15 mL). The organic phase was washed with 1 N NaOH (15 mL). The aqueous layers were combined, adjusted to pH 11 by the addition of 10% NaOH (3 mL), and extracted with $CHCl_3$ (3 × 15 mL). All of the organic layers were combined, dried over $MgSO_4$, filtered, and concentrated *in vacuo* to give a mixture of amines **5a** and **5b** as an orange oil (0.136 g, 0.819 mmol, 100% yield). TLC in CH_2Cl_2: R_f = 0.10 (one spot); ^{1}H NMR (300 MHz, $CDCl_3$) **5a**: δ 8.18 (d, J = 8.8 Hz, 2H), 7.53 (d, J = 8.4 Hz, 2H), 4.26 (q, J = 6.5 Hz, 1H), 1.42 (d, J = 6.5 Hz, 3H); **5b**: δ 7.79 (dd, J = 5.0, 1.4 Hz, 1H), 7.76 (dd, J = 5.0, 1.4 Hz, 1H), 7.60 (ddd, J = 7.8, 7.6, 1.0 Hz, 1H), 7.36 (ddd, J = 8.1, 7.3, 1.4 Hz, 1H), 4.60 (q, J = 6.5 Hz, 1H), 1.45 (d, J = 6.5 Hz, 3H); ^{13}C NMR (75 MHz, $CDCl_3$) **5a**: δ 149.0, 147.0, 126.8, 123.8, 50.9, 25.8; **5b**: δ 155.2, 142.0, 133.2, 127.7, 127.6, 124.0, 46.1, 24.7; ESI MS calc. 166.0, obs. $[M+H]^+$ 167.1.

N-((*S*)-1-(2-nitrophenyl)ethyl)acetamide (6)

A mixture of amines **5a** and **5b** (3.23 g, 19.48 mmol) and diisopropylethylamine (10 mL, 58.4 mmol, 3 equiv) was stirred at 0 °C, and acetic anhydride (4.60 mL, 48.7 mmol, 2.5 equiv) was added dropwise to the solution over 20 min. The reaction mixture was stirred for 3 h, during which time it was allowed to come to rt. The reaction mixture was cooled to 0 °C, acidified by the addition of 1 N HCl (15 mL), and extracted with EtOAc (3 × 50 mL). The combined organic layers were washed with saturated $NaHCO_3$ (3 × 30 mL) and saturated NaCl (2 × 30 mL), dried over Na_2SO_4, and concentrated *in vacuo* to yield a red-brown oil (4.02 g, 19.30 mmol, 99%). This material was 40% *ortho* isomer **6** (as determined by ^{1}H NMR integration). The *ortho* isomer was isolated by partial recrystallization from EtOAc. Briefly, the 4 g mixture of isomers was repeatedly dissolved in EtOAc (4 × 4 mL). The *para* isomer was fully soluble in this volume of EtOAc, while the *ortho* isomer (**6**) was insoluble and formed pale yellow needles that could be isolated in 96% purity (as determined by HPLC integration at 220 nm). TLC in EtOAc: R_f = 0.38; ^{1}H NMR (300 MHz, $CDCl_3$) δ 7.86 (dd, J = 8.3, 1.3 Hz, 1H), 7.57 (ddd, J = 7.7, 7.0, 1.3 Hz, 1H), 7.50 (dd, J = 7.7, 1.5 Hz, 1H), 7.39 (ddd, J = 8.3, 7.0, 1.5 Hz, 1H), 6.15 (bs, 1H), 5.48 (p, J = 7.1 Hz, 1H), 1.96 (s, 3H), 1.54 (d, J = 7.1 Hz, 3H); ^{13}C NMR (75 MHz, $CDCl_3$) δ 169.5, 148.8, 138.9, 133.5, 128.8, 128.2, 125.1, 46.8, 23.3, 21.5. ESI MS calc. 208.0, obs. $[M+H]^+$ 209.2.

(*S*)-1-(2-nitrophenyl)ethanamine hydrochloride (5b)

Acetamide **6** (0.206 g, 0.989 mmol) was refluxed in 5% aqueous HCl (10 mL) for 14 h. The reaction mixture was concentrated *in vacuo* to a yellow oil, which crystallized upon addition of diethyl ether. The diethyl ether was removed, and the residue was dried *in vacuo* to give **5b** as a yellow crystalline solid (0.200 g, 0.988 mmol, 99% yield). ^{1}H NMR (300 MHz, CD_3OD): δ 8.101 (dd, J = 7.6, 0.9 Hz, 1H), 7.838 (m, 2H), 7.685 (ddd, J = 8.4, 6.4, 2.3 Hz, 1H), 5.010 (q, J = 6.7 Hz, 1H), 1.730 (d, J = 6.8 Hz, 3H); ^{13}C NMR (75 MHz, CD_3OD): δ 150.3, 135.6, 134.0, 131.6, 129.0, 126.6, 47.5, 20.2; IR (cm^{-1}): 3406 (broad), 2885, 1601, 1534, 1341, 1096, 857; ESI MS calc. 167.1, obs. $[M]^+$ 167.1. m.p. (HCl salt): 184–188 °C. $[\alpha_D]^{25}$ (CH_3OH, c = 0.016): +2.812°

Peptoid Synthesis

Peptoids were synthesized on polystyrene resin with an Fmoc-protected Rink amide linker (0.69 mmol/g) using a modified version of our previously reported, μW-assisted peptoid synthesis method.[14] The resin Fmoc group was deprotected by soaking the resin (60 mg, 0.041 mmol) in a 20% piperidine/DMF solution (1 mL) for 20 min at rt, after which the resin was washed with DMF (5 × 1 mL) and drained. This deprotection procedure was repeated (1×). A solution of bromoacetic acid (0.10 g, 0.81 mmol, 20 equiv) and DIC (0.12 mL, 0.81 mmol, 20 equiv) in DMF (1 mL) was added to the deprotected resin (60 mg, 0.041 mmol, 1 equiv). The reaction mixture was heated with stirring in a commercial μW reactor to 35 °C in 30 s. The reaction mixture was filtered, and the resin was washed with DMF (5 × 1 mL) and drained. A solution of amine (spe, s2ne (**5b**), or snp; 0.81 mmol, 20 equiv) in DMF (1 mL) was added to the resin, and the mixture was heated with stirring in the μW reactor to 95 °C in 90 s for spe, or at 60 °C for 1 h (with 1 min ramp time) for s2ne and snp. The reaction mixture was filtered, and the resin was washed with DMF (5 × 1 mL) and drained. This two-step sequence of acylation and amination was repeated for the coupling of subsequent peptoid residues to generate peptoid nonamers. The resin-bound nonamers were washed with CH_2Cl_2 (4 × 1 mL) and drained. The peptoids were cleaved from the resin by stirring in 95% trifluoroacetic acid/H_2O (0.5 mL) for 20 min at rt. The resin was filtered and washed with CH_2Cl_2 (2 × 0.5 mL), and the filtrate was concentrated under N_2 to yield the peptoids as pale pink oils. Purity was determined by HPLC (UV detection at 220 nm), and the product identity was confirmed by MALDI-TOF MS. The peptoids were purified by preparatory HPLC to >95% purity before CD and NMR analyses.

X-ray crystallography

X-ray crystallography was performed on a CCD diffractometer with Mo K_α (λ = 0.71073 Å) radiation. Crystal data for acetamide **6**: $C_{10}H_{12}N_2O_3$, M = 208.22, tetragonal, a = 7.9423(19) Å, b = 7.9423(19) Å, c = 16.974(9) Å, U = 1070.7(6) $Å^3$, T = 100(2) K, space group $P4_3$, Z = 4, μ(Mo-Ka) = 0.097 mm^{-1}, 2954 reflections measured, 1114 unique (R_{int} = 0.1140) which were used in all calculations. The final $wR(F^2)$ was 0.0892 (all data). See Supporting Information for full details.

CD Analyses

Circular dichroism (CD) spectra were obtained on a digital spectropolarimeter at 24 °C. Peptoid stock solutions were prepared by dissolving at least 2 mg of each peptoid in spectroscopic grade acetonitrile. The stock solutions were diluted with spectroscopic grade acetonitrile to the desired concentration (60 μM) by mass using a high-precision balance. CD spectra were obtained in a square quartz cell (path length 0.1 cm) using a scan rate of 100 nm/min, with five averaged scans per spectrum. The spectrum of an acetonitrile blank was subtracted from the raw CD data, and the resulting data were plotted using Microsoft Excel 2004.

NMR Analyses

The heteronuclear single quantum coherence adiabatic (HSQCAD) NMR experiment[31] for **7** was performed on a 600 MHz NMR spectrometer using a 5 mm hcn probe. The data were

processed using the Varian VNMR software package (v. 6.1C). Peptoid **7** was dissolved in dimethylsulfoxide-d_6 to give a ~4 mM solution and transferred to a 5 mm NMR tube. The experiment was performed at 24 °C using the following parameter values: spectral widths were 6913.8 Hz in the ^{1}H dimension and 28622.5 Hz in the ^{13}C dimension. The number of transients (nt) and number of increments (ni) were 24 and 400, respectively. The number of points (np) was 2048. Square cosine window functions were applied in both dimensions. The spectra were zero-filled to generate f1 × f2 matrices of 4096 × 2048 points.

The 2D NOESY NMR experiment for **9** was performed on a 600 MHz NMR spectrometer using a 5 mm hcn probe. The data were processed using the Varian VNMR software package (v. 6.1C) and visualized using SPARKY software.[32] Peptoid **9** was dissolved in acetonitrile-d_3 to give a ~1 mM solution and placed in a 5 mm Shigemi NMR tube that was susceptibility-matched for dimethylsulfoxide. The 2D NOESY experiment was performed at 24 °C using the following parameter values: spectral widths were 8200.1 Hz in both ^{1}H dimensions. The number of transients (nt) and number of increments (ni) were 24 and 325, respectively. The number of points (np) was 2086, and 512 points were obtained by linear prediction in the f1 dimension. Square cosine window functions were applied in both dimensions. The spectra were zero-filled to generate f1 × f2 matrices of 4096 × 2048 points.

Supplementary Material

Refer to Web version on PubMed Central for supplementary material.

Acknowledgments

We thank the NSF (CHE-0449959), Burroughs Wellcome Fund, Research Corporation, Johnson & Johnson, and 3M for financial support of this work. H.E.B is an Alfred P. Sloan Foundation fellow. S.A.F. acknowledges the ACS Division of Medicinal Chemistry for a pre-doctoral fellowship (sponsored by Sanofi-Aventis) and Pfizer Global R&D for a Diversity in Organic Chemistry Fellowship. R. L. thanks the Faculty of Science at Mahidol University (Thailand) for an Undergraduate Student Degree Honor Program scholarship. Support for the NMR facilities at UW-Madison by the NIH (1 S10 RR13866-01 and 1 S10 RR08389-01) and the NSF (CHE-0342998 and CHE-9629688) is gratefully acknowledged. We thank Prof. Annelise Barron for the coordinates for the peptoid images in Figure 1; these molecular graphics images were produced using the UCSF Chimera package from the Resource for Biocomputing, Visualization, and Informatics at the University of California, San Francisco (supported by NIH P41 RR-01081). We also thank Dr. Charlie Fry and Dr. Monika Ivancic for assistance with NMR experiments, Dr. Ilia Guzei for X-ray crystallographic analyses, and Dr. Benjamin Gorske and Dr. Matthew Bowman for contributive discussions.

References and Notes

1. (a) Zuckermann RN, Kerr JM, Kent SBH, Moos WH. J Am Chem Soc. 1992; 114:10646–10647.(b) Patch, JA., Kirshenbaum, K., Seurynck, SL., Zuckermann, RN., Barron, AE. Pseudopeptides in Drug Development. Nielsen, PE., editor. Wiley-VCH; Weinheim, Germany: 2004. p. 1-31.
2. Xiao XS, Yu P, Lim HS, Sikder D, Kodadek T. J Comb Chem. 2007; 9:592–600. [PubMed: 17530904]
3. Hara T, Durell SR, Myers MC, Appella DH. J Am Chem Soc. 2006; 128:1995–2004. [PubMed: 16464101]
4. Chongsiriwatana NP, Patch JA, Czyzewski AM, Dohm MT, Ivankin A, Gidalevitz D, Zuckermann RN, Barron AE. Proc Natl Acad Sci U S A. 2008; 105:2794–2799. [PubMed: 18287037]
5. Seurynck-Servoss SL, Dohm MT, Barron AE. Biochemistry. 2006; 45:11809–11818. [PubMed: 17002281]

6. (a) Armand P, Kirshenbaum K, Falicov A, Dunbrack RL Jr, Dill KA, Zuckermann RN, Cohen FE. Fold Des. 1997; 2:369–375. [PubMed: 9427011] (b) Lee BC, Chu TK, Dill KA, Zuckermann RN. J Am Chem Soc. 2008; 130:8847–8855. [PubMed: 18597438]
7. (a) Kirshenbaum K, Barron AE, Goldsmith RA, Armand P, Bradley EK, Truong KT, Dill KA, Cohen FE, Zuckermann RN. Proc Natl Acad Sci U S A. 1998; 95:4303–4308. [PubMed: 9539732] (b) Wu CW, Sanborn TJ, Zuckermann RN, Barron AE. J Am Chem Soc. 2001; 123:2958–2963. [PubMed: 11457005]
8. (a) Armand P, Kirshenbaum K, Goldsmith RA, Farr-Jones S, Barron AE, Truong KTV, Dill KA, Mierke DF, Cohen FE, Zuckermann RN, Bradley EK. Proc Natl Acad Sci U S A. 1998; 95:4309–4314. [PubMed: 9539733] (b) Wu CW, Kirshenbaum K, Sanborn TJ, Patch JA, Huang K, Dill KA, Zuckermann RN, Barron AE. J Am Chem Soc. 2003; 125:13525–13530. [PubMed: 14583049]
9. Wu CW, Sanborn TJ, Huang K, Zuckermann RN, Barron AE. J Am Chem Soc. 2001; 123:6778–6784. [PubMed: 11448181]
10. Huang K, Wu CW, Sanborn TJ, Patch JA, Kirshenbaum K, Zuckermann RN, Barron AE, Radhakrishnan I. J Am Chem Soc. 2006; 128:1733–1738. [PubMed: 16448149]
11. Pettersen EF, Goddard TD, Huang CC, Couch GS, Greenblatt DM, Meng EC, Ferrin TE. J Comput Chem. 2004; 25:1605–1612. [PubMed: 15264254]
12. Shin SBY, Yoo B, Todaro LJ, Kirshenbaum K. J Am Chem Soc. 2007; 129:3218–3225. [PubMed: 17323948]
13. Pokorski JK, Miller Jenkins LM, Feng H, Durell SR, Bai Y, Appella DH. Org Lett. 2007; 9:2381–2383. [PubMed: 17506576]
14. Gorske BC, Jewell SA, Guerard EJ, Blackwell HE. Org Lett. 2005; 7:1521–1524. [PubMed: 15816742]
15. Gorske BC, Bastian BL, Geske GD, Blackwell HE. J Am Chem Soc. 2007; 129:8928–8929. [PubMed: 17608423]
16. Gorske BC, Blackwell HE. J Am Chem Soc. 2006; 128:14378–14387. [PubMed: 17076512]
17. Fowler SA, Stacy DM, Blackwell HE. Org Lett. 2008; 10:2329–2332. [PubMed: 18476747]
18. We utilize the previously established nomenclature for this peptoid residue (Nsnp) for clarity. See ref. 7a.
19. (a) Perry CW, Brossi A, Deitcher KH, Tautz W, Teitel S. Synthesis. 1977:492–494.(b) Nieuwenhuijzen JW, Grimbergen RFP, Koopman C, Kellogg RM, Vries TR, Pouwer K, van Echten E, Kaptein B, Hulshof LA, Broxterman QB. Angew Chem Int Ed. 2002; 41:4281–4286.
20. Walker JW, McCray JA, Hess GP. Biochemistry. 1986; 25:1799–1805. [PubMed: 3707910]
21. Salerno CP, Magde D, Patron AP. J Org Chem. 2000; 65:3971–3981. [PubMed: 10866616]
22. We also were able to synthesize s2ne (5b) from 2′-nitroacetophenone via a selective reduction of the ketone to the R-alcohol, conversion to the S-azide, and reduction to the S-amine, similar to the work of Gorske et al (see ref 16) However, the overall yield of 5b was significantly lower using this approach (12%, data not shown)
23. Coe JW, Brooks PR, Vetelino MG, Wirtz MC, Arnold EP, Huang J, Sands SB, Davis TI, Lebel LA, Fox CB, Shrikhande A, Heym JH, Schaeffer E, Rollema H, Lu Y, Mansbach RS, Chambers LK, Rovetti CC, Schulz DW, Tingley FD III, O'Neill BT. J Med Chem. 2005; 48:3474–3477. [PubMed: 15887955]
24. Bergeron RJ, McManis JS. J Org Chem. 1988; 53:3108–3111.
25. The quantity of acetamide 6 isolated by crystallization equaled the quantity of trifluoroacetamide 4b formed. Purity was assessed by ^{1}H NMR (>95%) and HPLC (96% purity at 220 nm).
26. We synthesized and characterized an *ortho*-methyl analog of peptoid 9 as a steric control. As (*S*)-1-(2-methylphenyl)ethylamine was not commercially available, we utilized 2-methylbenzylamine (2mb) for this control peptoid (*N*2mb(*N*spe)$_9$). The removal of the α-methyl group on the *N*-terminal side chain in this peptoid (and in similar nonamers we have studied) appears to strengthen the threaded loop (data not shown). We believe this may be due to an electronic effect, as the lack of an α-methyl group should decrease electron density at the *N*-terminal ammonium. Since we were unable to make direct comparisons between the control *N*2mb(*N*spe)$_9$ and peptoid 9, we omit this relatively complex analysis here for brevity.

27. We note that DMSO may be able to disrupt hydrogen bonding in a threaded loop-type structure (based on a qualitative comparison of the NMR spectra of 2 in acetonitrile-d_3 and DMSO-d_6; see Supporting Information). Therefore, the *cis:trans* ratio determined for 7 may be higher in DMSO relative to acetonitrile. We include the DMSO-d_6 data here to provide our most comprehensive analysis of peptoid 7.

28. Similar blue shifts in CD spectra for peptoids containing *N*snp residues have been observed previously; see ref 7a.

29. for a space-filling model of the threaded loop structure adopted by nonamer 2, see Figure 4 in ref. 10.

30. Assignments in the 1D ^{1}H NMR spectrum for 9 were corroborated by 2D NOESY data. See Supporting Information for 1D ^{1}H NMR spectrum of peptoid 9.

31. Boyer RD, Johnson R, Krishnamurthy K. J Magn Reson. 2003; 165:253–259. [PubMed: 14643707]

32. Goddard, TD., Kneller, DG. SPARKY v 3.112. University of California; San Francisco, CA:

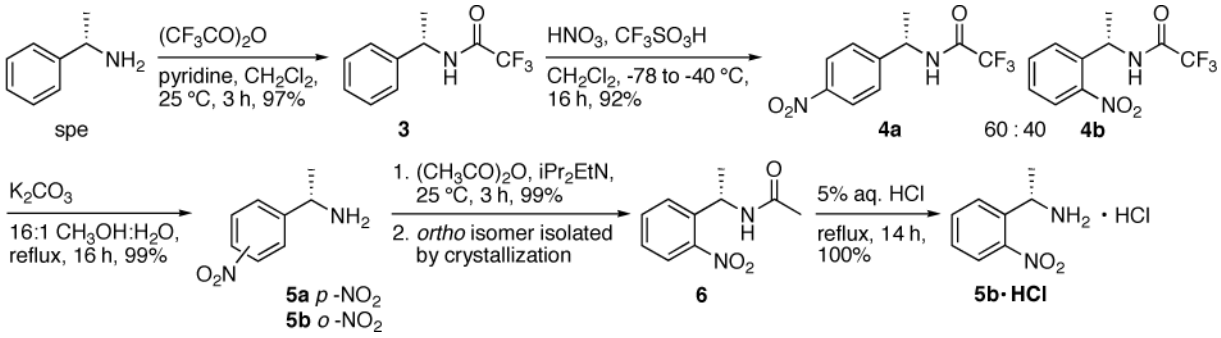

Scheme 1.

Synthesis of (*S*)-1-(2-nitrophenyl)ethanamine (s2ne, **5b**)

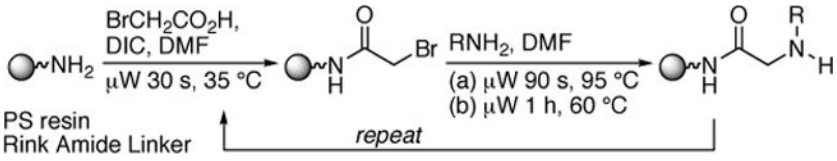

Scheme 2.

Microwave-assisted peptoid submonomer synthesis

Notes: S_N2 reaction conditions are (a) for amine spe, (b) for s2ne and snp. Oligomers are cleaved from the solid support by stirring in 95% TFA/H_2O for 20 min at rt. μW = microwave irradiation

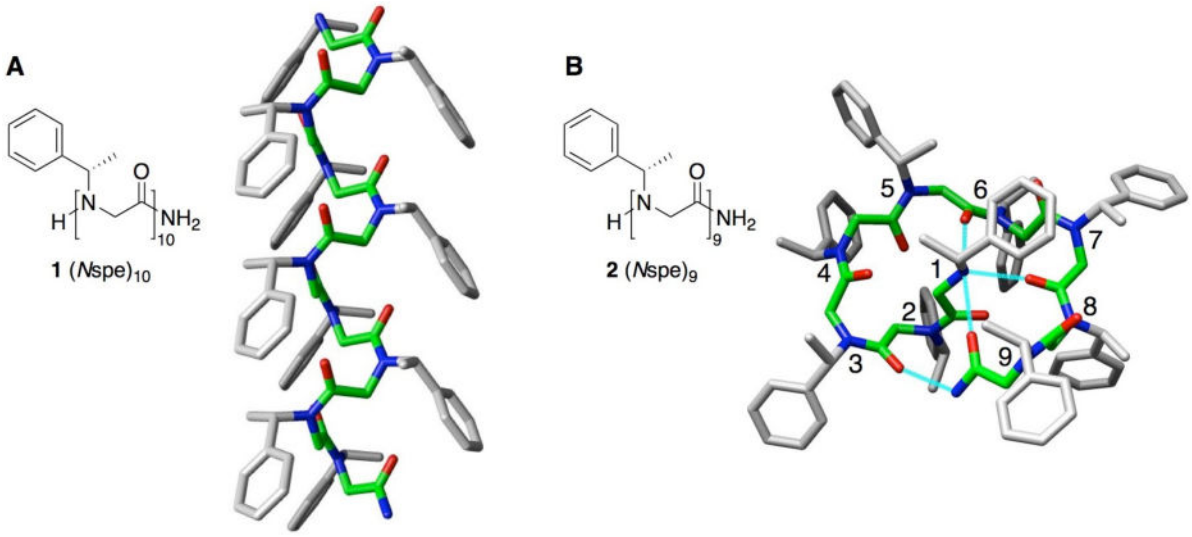

Figure 1.

A. The peptoid helix, shown here as the structure of $(N\text{spe})_{10}$ (**1**). Structure generated by molecular mechanics from the calculated structure of $(N\text{spe})_8$.[6a] Peptoid backbone highlighted in green. B. The peptoid threaded loop, shown here as the structure of $(N\text{spe})_9$ (**2**). Structure generated by solution-phase 2D NMR analyses.[10] Peptoid backbone highlighted in green and residues numbered sequentially from *N*-to *C*-terminus; intramolecular hydrogen bonds shown in cyan. 3D-images for helix and loop generated using Chimera (v. 1.2199).[11]

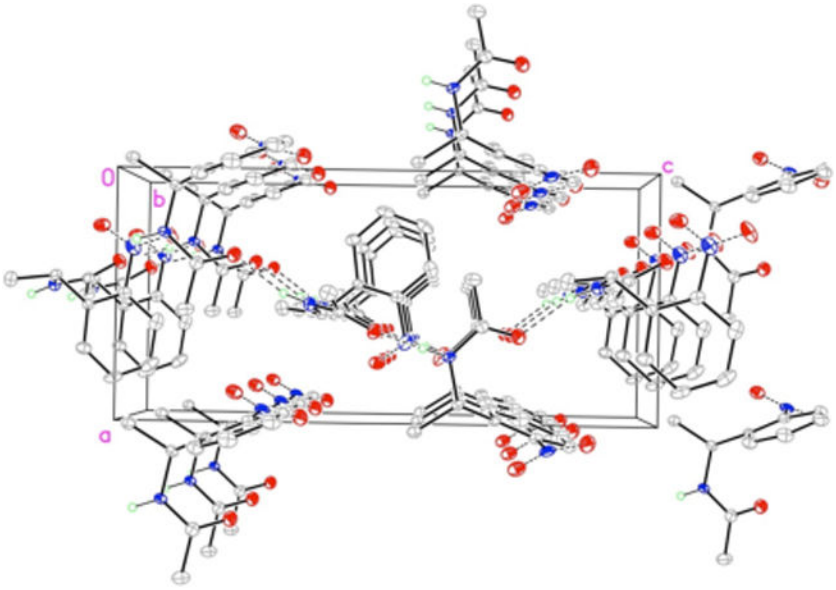

Figure 2.

X-ray crystal structure of acetamide **6**. The unit cell is indicated; intermolecular hydrogen bonds are shown in dashed grey.

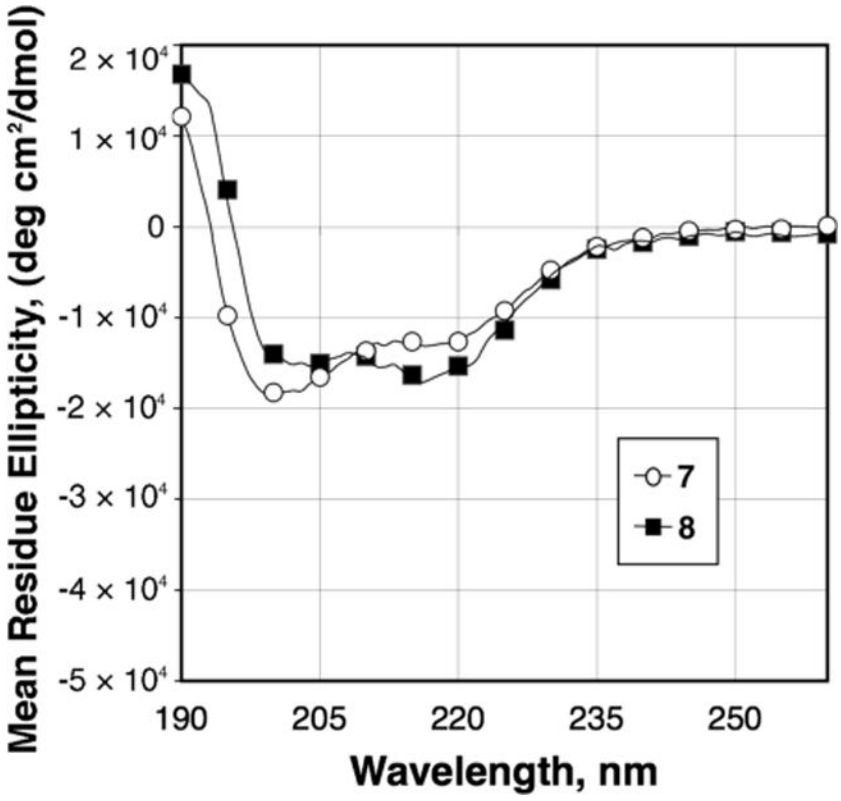

Figure 3.
CD spectra of peptoids **7** and **8** at 60 μM in acetonitrile. Spectra were collected at 24 °C.

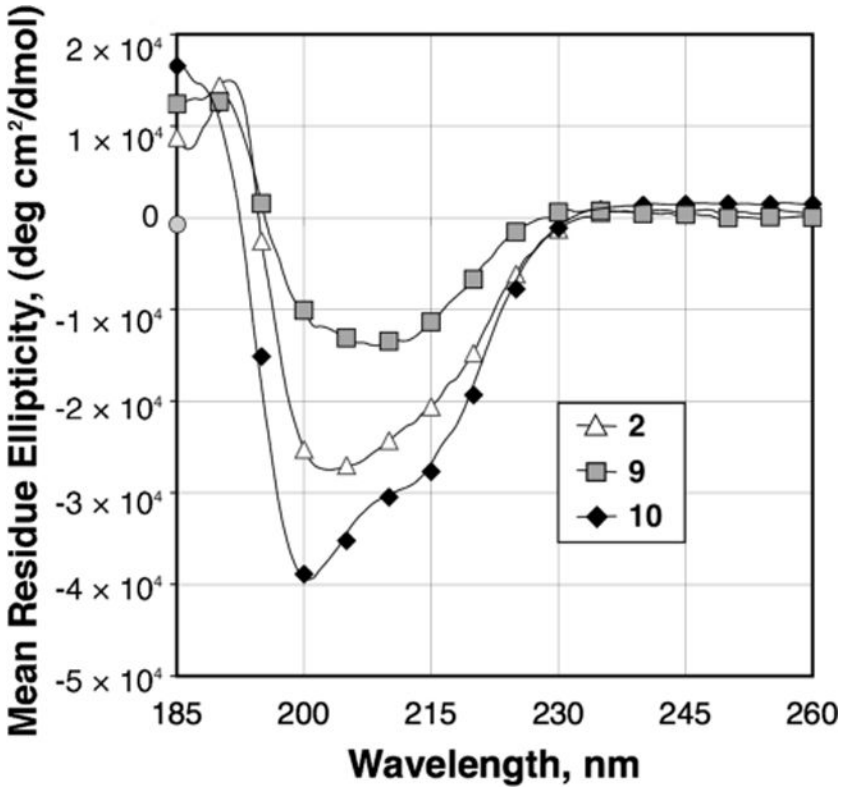

Figure 4.
CD spectra of peptoids **2**, **9**, and **10** at 60 μM in acetonitrile. Spectra were collected at 24 °C.

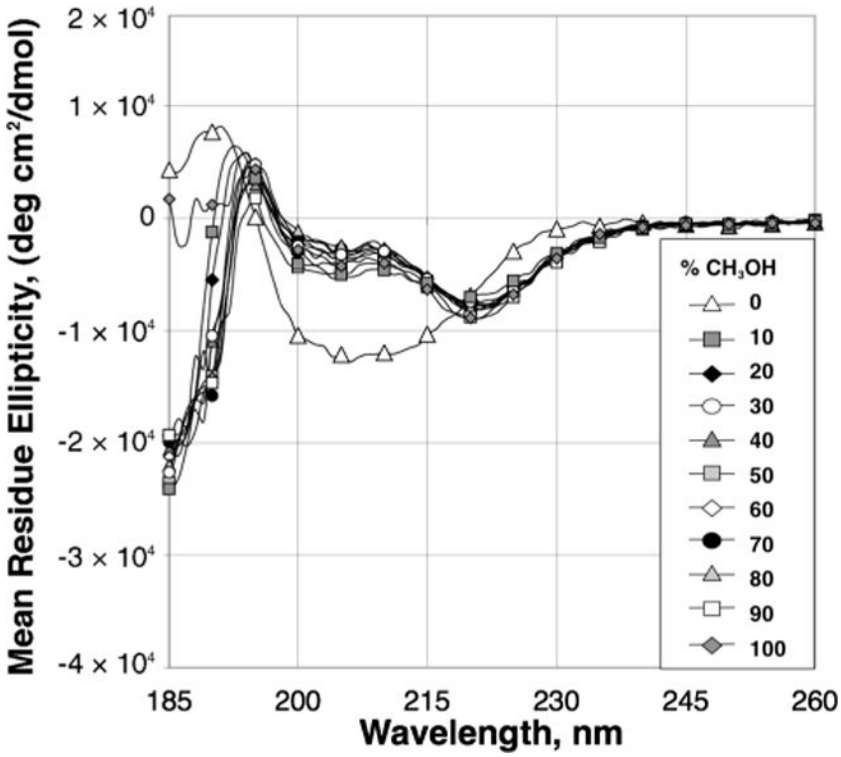

Figure 5.

CD spectra of peptoid **9** at 60 μM in acetonitrile/methanol solutions (0–100% methanol). Spectra were collected at 24 °C.

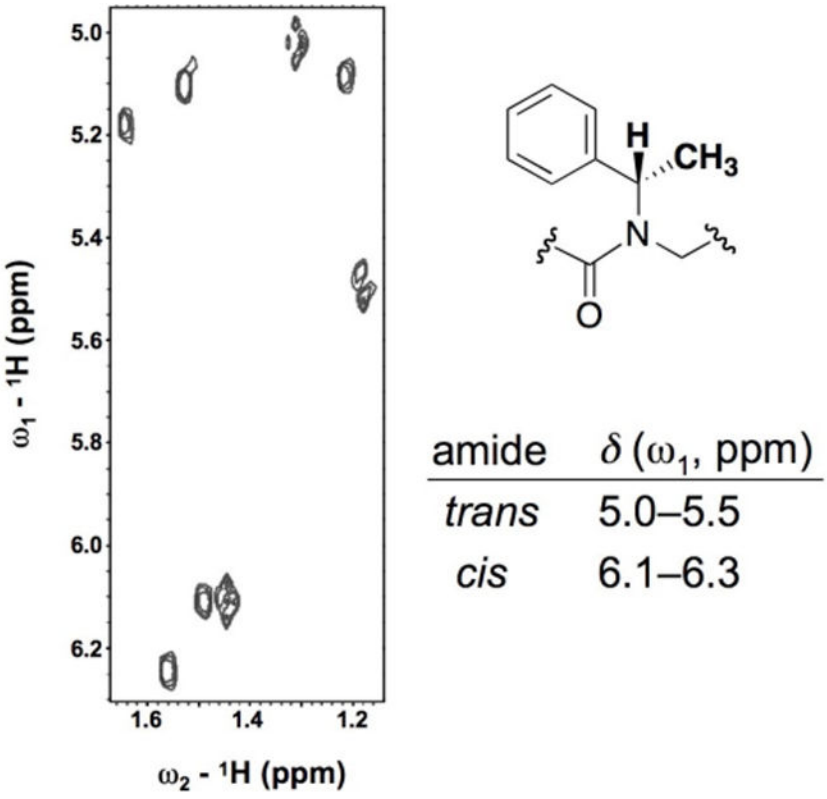

Figure 6.

Portion of a 2D NOESY spectrum of peptoid **9** showing correlations between benzylic H (ω_1) and CH_3 (ω_2). Ratio of amide rotamers = 1.2:1 *trans:cis*.

Table 1

Mass spectrometry data for peptoids **2** and **8**–**10**[a]

peptoid	calculated mass	observed mass (*m/z*)
2	1466.8	1468.3 $[M+H]^+$
8	1646.7	846.4 $[M+2Na]^{2+}$
9	1511.7	1535.5 $[M+Na]^+$
10	1511.7	1535.4 $[M+Na]^+$

[a]Peptoids purified to >95% purity before analysis by CD and NMR. Mass spectrometry data acquired using MALDI-TOF.